Modification of carbon nanotubes by a novel biomimetic approach towards the enhancement of the mechanical properties of polyurethane

Mu, Chenzhong; Zhang, Liying; Song, Yujie; Chen, Xuelong; Liu, Ming; Wang, Fuke; Hu, Xiao

2016

Modification of carbon nanotubes by a novel biomimetic approach towards the enhancement of the mechanical properties of polyurethane

Chenzhong Mu[a,b]，Liying Zhang[c], Yujie Song[b], Xuelong Chen[b], Ming Liu[c], Fuke Wang[d,*], Xiao Hu[b,*]

[a]*Energy Research Institute, Interdisciplinary Graduate School, Nanyang Technological University, Singapore 639798, Singapore*

[b]*School of Materials Science and Engineering, Nanyang Technological University, Singapore 639798, Singapore*

[c]*Temasek Laboratories, Nanyang Technological University, Singapore 639798, Singapore*

[d]*Department of synthesis and integration, Institute of materials research and engineering, A*STAR, Singapore 117602, Singapore*

[*]Corresponding authors. Tel: +65 6790 4610; Fax: +65 6790 9081

E-mail addresses: wangf@imre.a-star.edu.sg (F. Wang), ASXHU@ntu.edu.sg (X. Hu).

Abstract

Polyurethane (PU) nanocomposites incorporated with polydopamine treated carbon nanotubes (PDA-CNTs) were prepared by solution casting method *via* in-situ polymerization, achieving excellent CNT dispersion in the PU matrix. It was observed that, with a loading of only 0.3 wt%, the tensile modulus and tensile strength were increased by 40% and 100% respectively. This reinforcement even exceeded the predicted modulus by Halpin-Tsai model. It indicates extremely enhanced interfacial interaction between the fillers and the matrix. More

interestingly, it was found that the incorporation of PDA-CNTs caused a significant change in the degree of phase separation in the PU matrix leading to a unique network-like structure which is responsible for the unexpected reinforcement effect. This understanding combining with the synthetic approach should be useful for future design of PU/CNTs nanocomposites for a wide range of the applications.

Keywords:

Carbon nanotubes; Interface; Polymer nanocomposite

1. Introduction

The unique mechanical, electrical, magnetic, optical and thermal properties of carbon nanotubes (CNTs) make them ideal reinforcing agents for high performance polymer nanocomposites [1]. Since the first report of polymer nanocomposites using CNTs as a filler [2], CNTs enhanced polymer nanocomposites has become one of the most important research topics both in academic and industry R&D [3]. Various polymer matrices such as polystyrene, poly(ethyleneimine), epoxy, polyurethane, nylon 6 and polyethylene terephthalate have been used for composites with CNTs [4]. The presence of CNTs in polymer matrix can show remarkable enhancement of tensile strength, toughness, glass transition temperature and electrical conductivity [5].

Due to the strong Van der Waals force, CNTs tend to form bundles with each other and thus do not disperse well in the organic matrices in their pristine state. To achieve better dispersion and alignment of CNTs in organic matrix to improve the load transfer across the CNTs-polymer matrix interface, many approaches for functionalization of CNTs including oxidation, functional groups and other covalent functionalization have been developed [6, 7]. However, CNTs surface

functionalization approaches showed some obvious drawbacks such as tedious chemical reactions and high corrosive or toxic chemicals involvement. Most importantly, the surface modifications often lead to structure defects and fragmentation of the nanotubes, which remarkably decrease the mechanical and electronic properties of CNTs. Therefore, the non-covalent approaches were developed because these methods would not compromise the physical properties of CNTs but improve solubility and processability. The non-covalent approach mainly involves surfactants, biomacromolecules or wrapping with polymers [8, 9]. Although the non-covalent method is effective in isolation and debonding of CNTs, some problems still limit their wide applications. For instance, wrapping polymer with special structures required complicated chemical reactions with high cost. Also, the surfactants dispersion of CNTs could weaken the interfacial strength between CNTs and polymer matrix in general.

In the present work, we report the excellent dispersion of CNTs in polyurethane nanocomposites and exceptional enhancement of the tensile modulus and tensile strength by using polydopamine (PDA) coated CNTs. Motivated by mussel adhesive proteins [10], dopamine was found to form PDA layer on various types of materials including polymers, ceramic and metals through self-polymerization dopamine in aqueous solution [11, 12]. PDA coatings have been widely used in numerous materials for biomedical applications due to their physicochemical properties and strong surface adhesion abilities to various surfaces [13-15]. PDA is also employed as a functionalization modifier, e.g., anti-fouling coatings [16], nanofiltration for antibiotics removal [17], CO_2-philic for gas separation [18] and superhydrophobicity for oily water treatment [19]. Besides these PDA applications, secondary treatments can be easily achieved based on their intrinsic capacity, including inorganic Au [20], Ag [21] nanoparticles and CNTs-PDA/Co_3O_4 for Li-air batteries [22]. Moreover, PDA coating of

3

CNTs was reported to improve the dispersion of CNTs in various solvents or polymer matrices, recently [20, 23, 24]. However, current PDA studies are mainly focused on surface modification for improved biocompatibility and fabrication of hybrid materials for energy or catalytic applications. In the present work, we showed that PDA coated CNTs (PDA-CNTs) could successfully employ in polyurethane (PU) based polymer nanocomposites. We chose polyurethane (PU) as polymer matrix to demonstrate the concept because PU has been widely used in our daily life, e.g., in coatings, medical devices, adhesives, foams and so on [25]. Due to the good dispersion of CNTs in PU matrix and enhanced interfacial interaction between fillers and matrix, 40% and 100% increments of tensile modulus and tensile strength were obtained with 0.3 wt% loading of PDA-CNTs. The influence of PDA-CNTs on the structure of PU are explored and analysed in detail as well.

2. Experimental Section

2.1 Materials

The multi-walled carbon nanotubes (CNTs, Nanocyl™ NC 7000 with an average diameter of 9.5 nm and length of 1.5 μm) synthesized by chemical vapor deposition were purchased from Nanocyl S.A. Polyisocyanate (N3390 with the isocyanate content 19.6%, from Bayer Company), defoamer (BYK A535), anhydrous N, N-Dimethylformamide (DMF, 99.8% Sigma-Aldrich) and dibutyltin dilaurate (95% provided by Sigma-Aldrich) were used as received. Polyol (Capa 7203, hydroxyl value is 54 mg KOH/g) was dehydrated in vacuum oven at 110 $^{\circ}$C overnight before use. Cyclohexanone (ACS reagent, ≥99.0%) was dried at least 48 h by 4A molecular sieves before use. Dopamine hydrochloride (99%) and tris (hydroxymethyl)-aminomethane hydrochloride were purchased from Regent Chemicals Pte Ltd.

2.2 Preparation of PDA-CNTs

The procedure of PDA-CNTs preparation was mainly followed by the description in the literature [26, 27]. The slightly modified procedure was briefly described as below. 0.2 g CNTs was dispersed into DMF containing Tris buffer solution (pH 8.5) in ultrasonic bath. After formation of a homogeneous suspension, 2 mg/ml dopamine was added into CNTs/DMF suspension and the mixture of dopamine and CNTs was mildly magnetically stirred for 6 h at room temperature. The PDA-CNTs were obtained by repeating centrifugation and washed by deionized water for 3-4 times in order to remove unreacted dopamine monomers and free polydopamine. After that, the modified CNTs were dried by freeze dryer for 48 h. The pure polydopamine was also synthesized following the same procedure.

2.3 Fabrication of PU/CNTs nanocomposites

PU/PDA-CNTs nanocomposites were prepared *via* in-situ polymerization. Firstly, PDA-CNTs were ultrasonically dispersed into large amount of DMF for 2 h, followed by the addition of certain amount of polyisocyanate. Then, the mixture of polyisocyanate and PDA-CNTs was continuously stirred at 80 $^{\circ}$C for 2 h in nitrogen atmosphere. The obtained mixture concentrated by rotary evaporation was further added into a three-neck flask containing stoichiometric polyol and catalyst. Finally, PU/PDA-CNTs films were obtained by casting the solution onto a glass plate and subsequently removed the solvent at 60 $^{\circ}$C in vacuum for 24 h. The solid samples were kept for one week in dry box before the characterization. In this paper, the samples were defined as PU/PDA-CNTs X. For example, PU/PDA-CNTs 0.1 means PU nanocomposite containing 0.1 wt% PDA-CNTs. To compare the effects of pristine CNTs and PDA-CNTs, the same weight percentage of CNTs was used. For example, the weight percentage of pristine CNTs in PU/Pristine CNTs 0.3 is 0.24 wt%, which corresponds to the practical CNTs loading in PU/PDA-

CNTs 0.3. The isocyanate index (molar ratio of -NCO groups to -OH groups) used in this paper was fixed at 1.1:1 for neat PU, while the isocyanate indexes for PU/PDA-CNTs nanocomposites were slightly adjusted in order to optimize the properties of PU/PDA-CNTs nanocomposites [28]. The procedure of preparing PDA-CNTs and PU/PDA-CNTs nanocomposites is shown in **Scheme 1** and **Scheme 2**, respectively.

2.4 Characterizations:

Fourier transform infrared spectroscopy (FT-IR) was used to confirm the modification of CNTs by PDA and attenuated mode was employed to study hydrogen bonding within the hard domains and the degree of ordering of the hard segments in nanocomposites. The tests were carried out using Frontier FTIR/NIR spectrometer (PerkinElmer). A total of 32 scans were taken on each specimen with a resolution of 2 cm^{-1} between 650 and 4000 cm^{-1}. The carbonyl regions between 1800 and 1600 cm^{-1} were used to study hydrogen bonding in the hard domains. Thermogravimetrc analysis (TGA) was used to estimate the percentage of PDA on CNTs by Q500 (TA Instruments,). A typical specimen weight was 10 mg, placed in a platinum sample pan. Specimens were studied at a heating rate of 10 °C/min under an air atmosphere (balance gas: nitrogen 60 ml/min and sample gas: air 40 ml/min). Transmission electron microscopy (TEM) was employed to investigate the morphological structure of pristine CNTs and PDA-CNTs. Specimens were prepared by placing one droplet of diluted ethanol suspension on carbon-coated copper grid and dried at 60 °C for overnight. The TEM images were recorded on a JEOL 2010 TEM at 200 kV. The fracture surfaces of nanocomposites were investigated by using a field emission-scanning electron microscope (Jeol FESEM 7600F) at 5 kV. The fracture surfaces of nanocomposites were investigated by using a field emission-scanning electron microscope (Jeol FESEM 7600F) at 5 kV. The freeze fracture surfaces of specimens were prepared in liquid

nitrogen and a layer of platinum coating with a thickness of 20 nm was applied on the fracture surfaces in order to obtain clear images. Mechanical properties of the nanocomposites were evaluated by tensile test (Instron 5567). For tensile tests, the specimens were punched using ASTM D638-V dog bone die. The testing film had a gauge of length of 9.53 mm and width 3.52 mm. The crosshead speed was kept at 20 mm/min to measure the stress vs strain behavior of neat PU, PU/Pristine CNTs and PU/PDA-CNTs nanocomposites. Each nanocomposite with varied formulations was tested at least five specimens in order to obtain an average.

3. Results and discussion

3.1 Modification of CNTs by Polydopamine (PDA)

In this study, the as received pristine CNTs were used without any purification, in order to retain their intrinsic structure. The PDA coated CNTs (PDA-CNTs) were prepared by self-oxidative polymerization of dopamine in DMF solution (**as exhibited in Scheme 1**).

The successful PDA coating onto the surface of pristine CNTs was confirmed by comparing FTIR spectra of pristine CNTs and PDA-CNTs, as shown in **Fig. 1a**. It can be seen that pristine CNTs exhibited strong peaks at 3430 and 1400-1640 cm^{-1} due to the -OH groups and benzene rings [29], respectively. The presence of -OH group can be assumed to be the slight oxidation of CNTs when manufactured or moisture effect [30]. Compared with pristine CNTs, some new peaks appeared after being coated by PDA layers. The broad absorption band at 3424 cm^{-1} can be assigned to the overlap of -OH groups and -NH stretching vibrations [30]. In addition, the peaks at 2970, 2900 and 2857 cm^{-1} are attributed to aliphatic C-H vibration stretching modes, and the characteristic peak at 1739 cm^{-1} is assigned to carbonyl groups. Moreover, another two new peaks clearly appeared at 1540 and 1378 cm^{-1} that are assigned to -C=N and -C-N-C,

7

respectively [31]. The presence of these new peaks confirms that PDA was successfully coated onto CNTs through the simple oxidative-polymerization method.
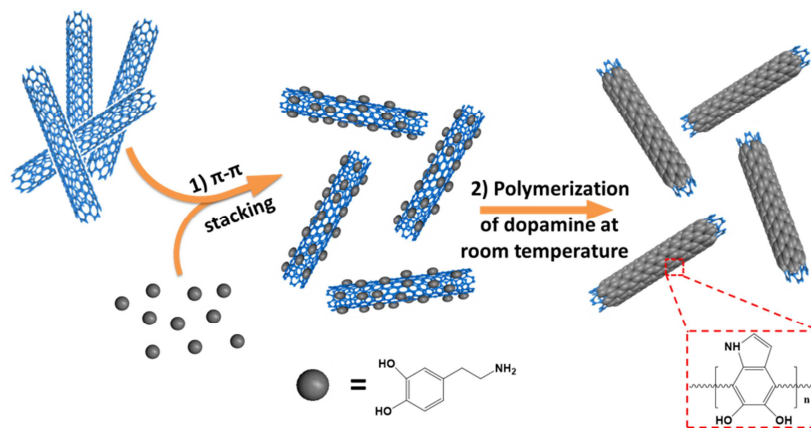
Scheme 1. Schematic illustration for the preparations of PDA-CNTs.

To quantify the amount of PDA coated on the CNTs, TGA tests of pristine CNTs and PDA-CNTs were performed. As shown in **Fig. 1b**, the weight loss of PDA-CNTs was more obvious than that of pristine CNTs, which arises from the degradation of PDA. From the TGA curve of pristine CNTs, the onset degradation temperature of CNTs was found about 493 $^{\circ}$C. Meanwhile, the weight residue of PDA-CNTs was 85.1% at 493 $^{\circ}$C. Accordingly, the approximation of weight percentage of PDA covered over CNTs was calculated to be ~15%.

The thickness and morphology of the CNTs before and after modification were examined by transmission electron microscopy (TEM). It can be seen from **Fig. 2**, the diameter of pristine CNTs with a smooth surface is between 10-20 nm. After modification, the CNTs were covered by a layer of PDA with the thickness of ~1-2 nm, as seen in **Fig. 2b**. The low magnified TEM picture indicates that the PDA layers were uniformly covered onto the CNTs.
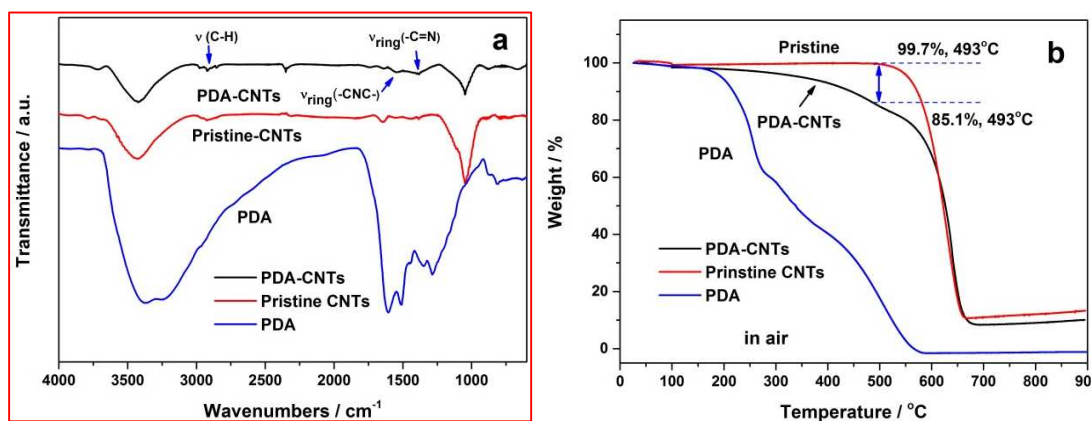
Fig. 1. (a) FTIR spectra and (b) TGA curves of pristine CNTs, PDA-CNTs and pure PDA.
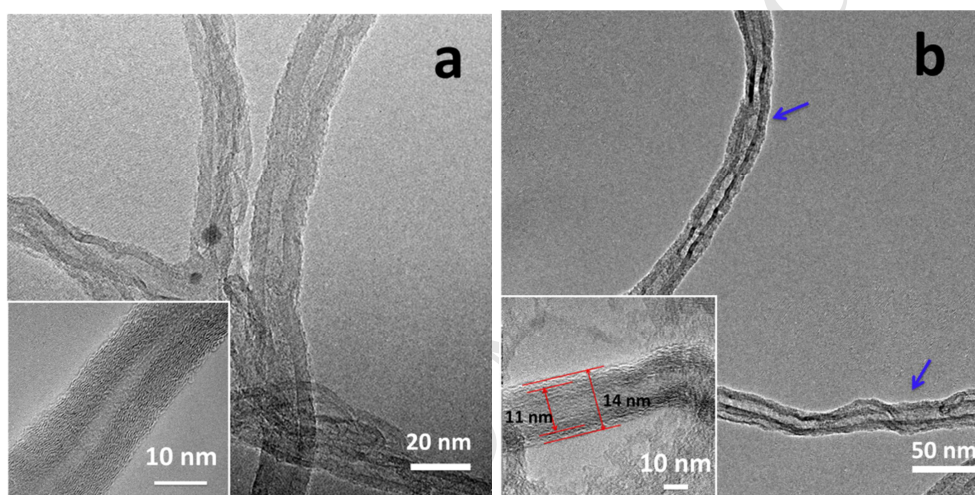

Fig. 2. TEM images of (a) pristine CNTs and (b) PDA-CNTs. Arrows show the PDA coating wrapped on the nanotubes. The high magnified pictures with a scale bar at 10 nm were given for better clarity.

3.2 Mechanical properties of PU/PDA-CNTs nanocomposites

PDA-CNTs were incorporated into PU matrix *via* in-situ polymerization to study the influences of PDA-CNTs on PU nanocomposites. The PDA-CNTs were firstly added into polyisocyanate and followed by reacting with polyol, in order to avoid the adverse interference of competing reactions between polyol and PDA-CNTs with polyisocyanate.

The mechanical properties of neat PU and PU/PDA-CNTs nanocomposites were investigated by tensile testing. The representative tensile stress-strain curves and mechanical properties are

shown in **Fig. 3a**. With the incorporation of PDA-CNTs, the mechanical properties were increased for all formulations except the Young's modulus of the nanocomposite with 0.5 wt% PDA-CNTs loading. Noticeably, the maximum increment of Young's modulus and tensile strength was reached at only 0.3 wt% PDA-CNTs loading, i.e., the Young's modulus and tensile strength were increased by 40% (from 0.9 MPa for neat PU to 1.3 MPa for PU/PDA-CNTs 0.3) and 100% (from 1.1 MPa for neat PU to 2.2 MPa for PU/PDA-CNTs 0.3), respectively. Moreover, the elongation at break for nanocomposites with 0.1 wt% and 0.3 wt% of PDA-CNTs also increased. It is explained that the presence of uniform PDA coatings can help release the interfacial stress concentration, leading to effectively stress transfer between the polymer and CNTs [32, 33]. The Young's modulus decreased upon further increasing the PDA-CNTs loading to 0.5 wt% (from 0.9 MPa for neat PU to 0.6 MPa for PU/PDA-CNTs 0.5). The decreased Young's modulus of nanocomposite with 0.5 wt% PDA-CNTs might arise from the aggregation of PDA-CNTs. The PDA-CNTs play multi roles in the resulting nanocompsites, e.g., fillers, chain extender and crosslinkers. As crosslinkers and chain extender to increase crosslinking density and higher molecular weight, PDA-CNTs can improve the modulus of the nanocomposites. While as reinforced fillers, the influence of PDA-CNTs on nanocomposites depends on the dispersion of PDA-CNTs in polymer matrix as well. The formation of PDA-CNTs aggregates or bundles occurred at the high content of PDA-CNTs.

To further investigate the enhancement of interfacial interaction, a PU/Pristine CNTs nanocomposite was prepared as a reference. The mechanical properties of PU/Pristine CNTs are shown in **Fig. 3b**. Young's modulus decreased significantly with the incorporation of pristine CNTs, while elongation at break increased accordingly. The decreased modulus can be attributed to the poor dispersion of pristine CNTs and disruption of reaction between isocyanate groups and

hydroxyl groups by pristine CNTs, which exhibit strong adsorption ability to various substances [8, 34, 35].

Fig. 3c shows the comparison of mechanical properties of the PU/modified CNTs by various methods nanocomposites with the results in this work, including alkoxysilane, acid and amine [36-38]. It is worth noting that tensile strength increased obviously in our work, even the PDA-CNTs loading in our work was only 0.3 wt%.
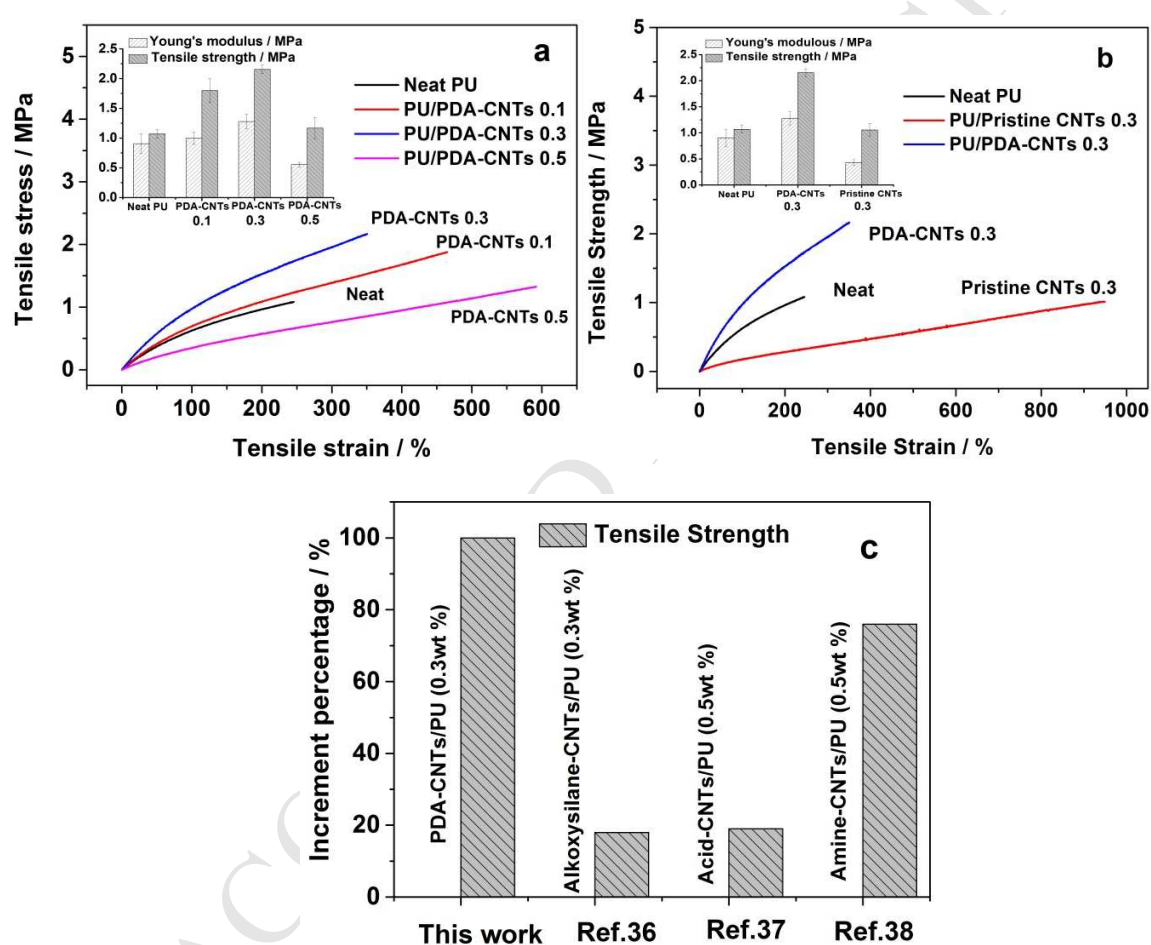

Fig. 3. (a) Tensile results of neat PU and PU/PDA-CNTs nanocomposites, (b) comparison of tensile results of PU/PDA-CNTs and PU/Pristine CNTs and (c) comparison of mechanical properties of the PU/modified CNTs by various methods nanocomposites with the results in this work. Inset histograms represent the comparison of Young's modulus and tensile strength.

3.3 Morphology and interfacial interaction between PU and CNTs nanocomposites

The fracture morphology and the dispersion of PDA-CNTs in PU matrix were examined by field emission scanning electron microscope (FESEM) as shown in **Fig. 4**. The fracture of neat PU exhibits a brain-like texture, which arises from the phase separation behavior. On the contrary, a spherulitic structure was observed in PU/PDA-CNTs 0.3, which was attributed to the enhanced phase separation. Moreover, PDA-CNTs could be found in "bump parts" assigned to hard domains, which indicates that PDA-CNTs were preferentially located in hard domains in PU matrix. This gives strong evidence that phase separation was increased by the addition of PDA-CNTs, which induced the formation of hard domains. It is also found that the PDA-CNTs were difficult to pull out from matrix, which is ascribed to the creation of interfacial bonding between CNTs and matrix, as shown in the inset of **Fig. 4b**. Further increasing the PDA-CNTs to 0.5 wt%, the unexpected aggregation of PDA-CNTs occurs, resulting in the decreased mechanical property (**Fig. 4c**). By comparison with pristine CNTs incorporation, we found that without PDA modification, the aggregation of pristine CNTs in PU matrix was serious, and the CNTs were easily pulled out, as shown in the inset of **Fig. 4d**.

To eliminate the influence of elastic deformation during tensile test and further gain a more clear visualization of the morphology, cryo-fracture surfaces were also examined. The defined phase separation was clearly observed for neat PU shown in **Fig. 4e**. The "flower" pattern might arise from the stretched orientation of hard domains when cracked. As expected, the defined spherulitic structure of PU/PDA-CNTs 0.3 was clearly observed to be a continuous network, as shown in **Fig. 4f**. In this study, the preparation of PDA-CNTs nanocomposites was followed by two steps method, in order to avoid competing reaction between PDA-CNTs and polyols. Firstly, PDA-CNTs reacted with polyisocyante, so that isocyanate terminated PDA-CNTs formed in the

12

first stage. Secondly, the mixture of polyisocyanate and isocyanate terminated PDA-CNTs were introduced into polyols. At this stage, polyols as polymer solvents dissolved the mixture of polyisocyante and isocyanate terminated PDA-CNTs as hard segments. As the reaction proceeded, hard segments would phase separate by nucleation and growth process to produce larger hard domains [39, 40], in which the nucleation was mainly benefited from PDA-CNTs as CNTs are good nucleating agent. The formed network of PDA-CNTs/PU nanocomposites is illustrated in **Scheme 2**.
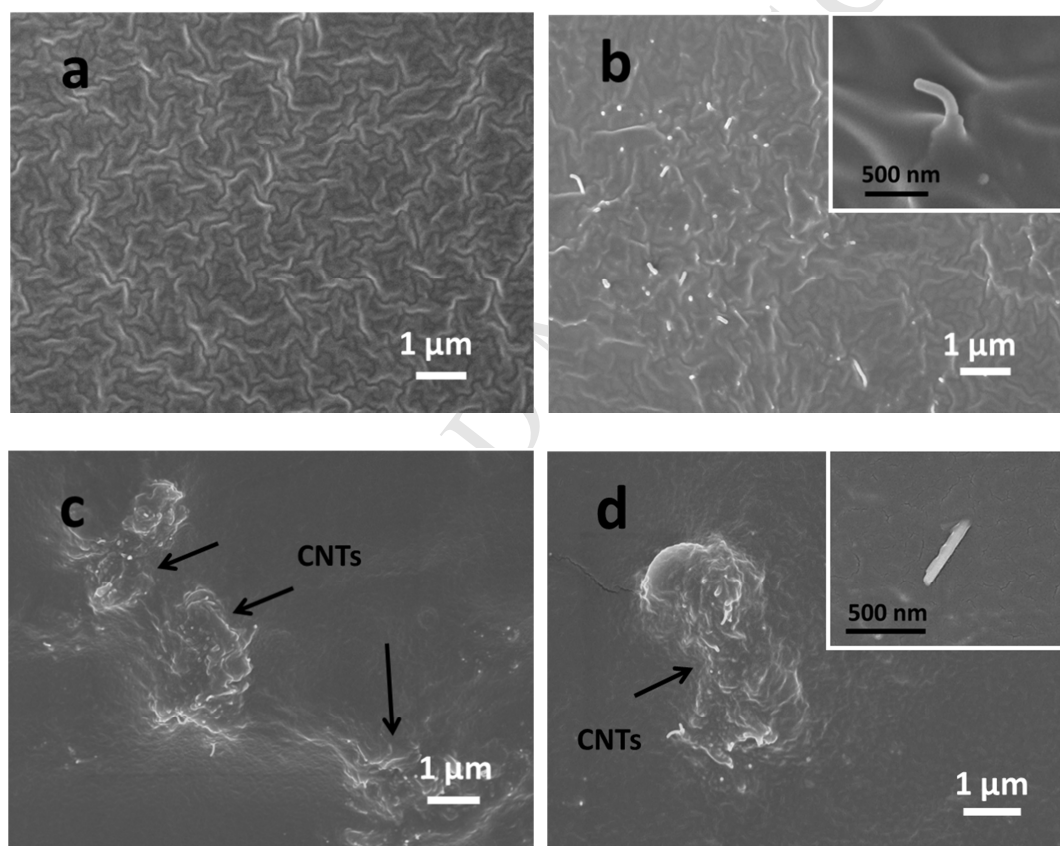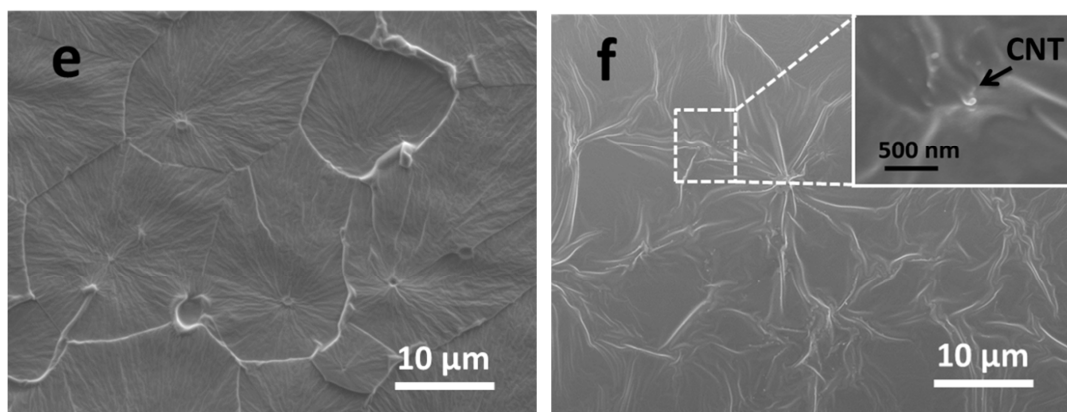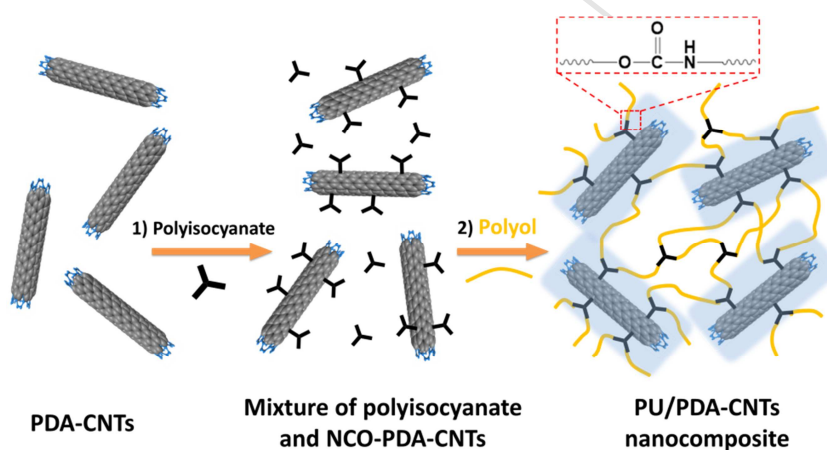
Fig. 4. SEM images of the fractures of (a) neat PU, (b) PU/PDA-CNTs 0.3, (c) PU/PDA-CNTs 0.5 and (d) PU/Pristine CNTs 0.3 after tensile test at room temperature and the cryo-fractures of (e) neat PU and (f) PU/PDA-CNTs 0.3. The insets are the high magnification pictures.

Scheme 1. Schematic illustration for network formation of PU/PDA-CNTs nanocomposites.

3.4 Phase separation of PU/PDA-CNTs nanocomposites

To further quantify the influence of PDA-CNTs on PU nanocmoposites, the degree of phase separation was investigated by FTIR technique. **Fig. 5a** shows the FTIR spectra of neat PU and PU/PDA-CNTs nanocomposites in the range 650-4000 cm^{-1}. It is obvious that there is no peak appearing at 2270 cm^{-1}, corresponding to free isocyanate groups. The absence of free -NCO peak and the appearance of urethane groups at around 3300, 1730 and 1680 cm^{-1} indicate the

completion of curing reaction [41]. However, no significant differences can be observed among these spectra, which could be attributed to the low content of CNTs and the wrapping effect of polyurethane matrix.

Typically, -C=O and -NH bands are commonly used to study the structure of polyurethane composites. The hydrogen bonding between -NH as proton donors and -C=O as proton acceptors is formed inside PU [42]. As a result of hydrogen bonding formation, three absorption peaks of -C=O can be detected at around 1730, 1700 and 1680 cm^{-1}, which correspond to non H-boned (free) carbonyl groups, H-boned carbonyl groups in disordered (amorphous phase) and H-boned carbonyl groups in ordered domains, respectively [43].

The carbonyl (-C=O) zone from 1600-1800 cm^{-1} was deconvoluted for polyurethane nanocomposites with different PDA-CNTs loadings. The degree of phase separation (DPS) of polyurethane nanocomposites can be calculated by using Equation [43]:

$$DPS = \frac{A_{disordered} + A_{ordered}}{A_{disordered} + A_{ordered} + A_{free}}$$

(1)

where *A* stands for the area of the peaks, while the subscripts of disordered, ordered and free mean disordered, ordered and free confirmations of carbonyl bonds. The deconvolution results of nanocomposites are shown in **Fig. 5b**.

It was found that the incorporation of 0.1 wt% PDA-CNTs loading increased the DPS slightly by ~3% (from 52% for neat PU to 55% for PU/PDA-CNTs 0.1 nanocomposite). The significantly increased DPS (~61%) was obtained when the PDA-CNTs content was up to 0.3 wt %. The increased DPS can be attributed to the formation of large amounts of urethane/urea groups on the surface of PDA-CNTs since PDA layers contains large amounts of amine groups (primary and secondary) and hydroxyl groups (the blue area in **Scheme 2**). Continuously increasing the PDA-CNTs loading, DPS decreased, but still higher than that of neat PU, for

15

example, the DPS was 57% for PU/PDA-CNTs 0.5. The decrease of DPS in PU/PDA-CNTs 0.5

is ascribed to the aggregation of CNTs. The calculated DPS results are well consistent with the
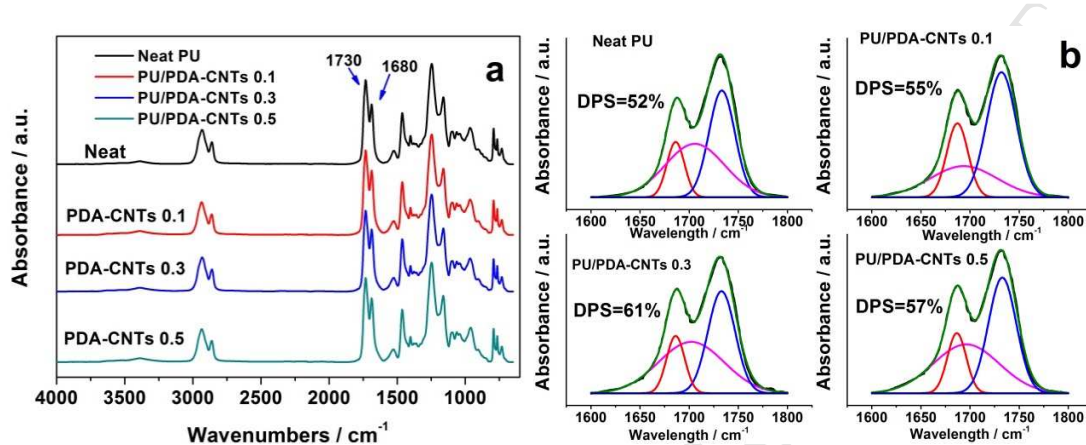
conclusion from SEM observations.

Fig. 5. (a) FTIR spectra of PU/PDA-CNTs nanocomposites and (b) deconvolution results of

FTIR spectra of the carbonyl group region for PU/PDA-CNTs nanocomposites.

3.5 Halpin-Tsai model calculation

To get a clear understanding on the reinforcement mechanism, we employed Halpin-Tsai

model to predict the modulus of unidirectional or randomly distributed PDA-CNTs reinforced

PU nanocomposites, which is the most widely used model to estimate reinforcement effect of

fillers in nanocomposites, e.g., CNTs. The Haipin-Tsai equations are expressed as follows [33,

44-46],

$$E_c = E_m[\frac{3}{8} * \frac{1+\eta_L\xi V_f}{1-\eta_L V_f} + \frac{5}{8} * \frac{1+2\eta_T V_f}{1-\eta_T V_f}] \tag{2}$$

$$E_{||} = E_m[\frac{1+\eta_L\xi V_f}{1-\eta_L V_f}] \tag{3}$$

$$\eta_L = \frac{(E_f/E_m)-1}{(E_f/E_m)+\xi} \tag{4}$$

$$\eta_T = \frac{(E_f/E_m)-1}{(E_f/E_m)+2} \tag{5}$$

16

$$\xi = 2a_f/3 = 2l_f/3t_f \tag{6}$$

where E_c and $E_{//}$ represent the Young's modulus of the nanocomposite with randomly distributed PDA-CNTs and the Young's modulus of the nanocomposite with fully aligned PDA-CNTs [45], respectively. The terms of η_L, η_T and ξ are used to simplify equations (2) and (3). η_L is related to the material properties of polymer and fillers, and geometry of nanofillers, while η_T is only dependent on the material properties of polymer and filler. ξ refers to the anisotropic nature of the fillers, i.e., aspect ratio. E_f and E_m are Young's modulus of the PDA-CNTs and the polymer matrix. a_f, l_f and t_f refer to the aspect ratio, length, and diameter of the carbon nanotubes, and V_f is the volume fraction of PDA-CNTs in the nanocomposites.

The Young's modulus of the CNTs was previously measured as about 270 GPa [47], which was used in this paper. The Young's modulus of pure PU was 0.9 MPa from the experimental data. The density of the PU matrix was 1.2 g/cm^3, and that of PDA-CNTs was 1.6 g/cm^3. The average l_f and d_f of CNTs are about 1.5 μm and 9.5 nm from the data sheet, respectively. **Fig. 6** shows the comparison between experimental results and calculation results.

It is worth noting that the moduli of the nanocomposites with 0.1 wt% and 0.3 wt% PDA-CNTs were 7% and 29% higher than predicted moduli (randomly distributed) respectively, even higher than those from aligned predictions. The dramatic reinforcement effect that the experimental modulus value greatly exceeded the model predictions can be explained by the combination of several factors in PU/PDA-CNTs nanocomposites. Firstly, the incorporation of PDA-CNTs increased the mechanical properties of nanocomposites as CNTs has extremely high modulus and aspect ratio of length and width. Secondly, large amounts of chemical linkages formed between polyurethane matrix and PDA-CNTs due to the rich reactive hydrogen-containing groups in PDA layers. The strong interfacial interaction (i.e., chemical bonding and

17

hydrogen bonding) also contributes to the reinforcement of PU/PDA-CNTs, which can effectively transmitted the external load from polymer matrix to CNTs through the interfacial PDA layers. Thirdly, phase separation of PU was increased by PDA-CNTs addition leading to a structural change, which was reflected by the formation of continuous network of hard domains. Thus, the excellent mechanical properties could be achieved for PU/PDA-CNTs nanocomposites by these synergistic effects. This unrivaled reinforcement effects that the moduli of nanocomposites were higher than the prediction by Halpin-Tsai model also were observed in GO nanocomposites by Morimmune et.al [48] and Liang et.al [49], as shown in **Fig. 6**. The phenomenon was attributed to the GO reinforcement and the interaction between polymer matrix (polyvinyl alcohol) and graphene oxide (GO). Therefore, it is reasonable that our experimental results were much higher than the predictions of theoretical model.
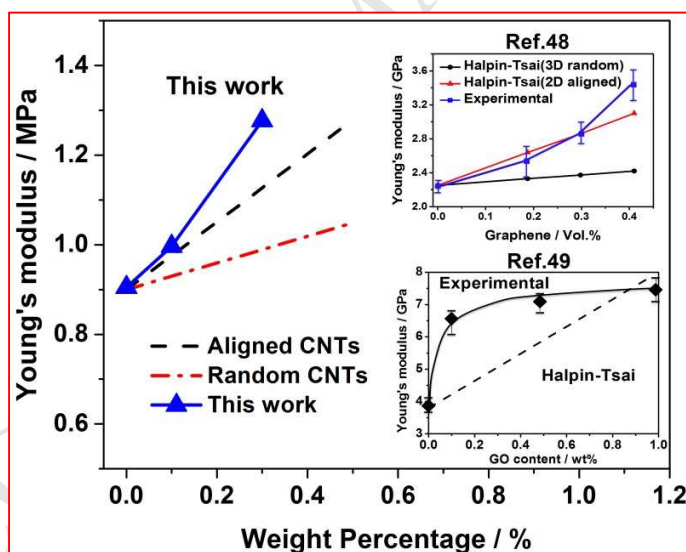

Fig. 6. Comparison between the calculated results using the Halpin-Tsai model and the experimental results.

4. Conclusion

The PDA-CNTs were prepared by a facile, eco-friendly method and successfully incorporated into polyurethane matrix. It was found that the incorporation of PDA-CNTs enhance the mechanical properties of PU/PDA-CNTs nanocomposites obviously. The PDA layer provided good dispersion of PDA-CNTs in polyurethane matrix and extremely high interfacial interaction between PDA-CNTs and polyurethane, which can effectively transfer load from polymer matrix to CNTs. Moreover, the preferential dispersion of PDA-CNTs in hard domains led to a significant change of degree of phase separation in the PU matrix. By comparison with pristine CNTs and PDA-CNTs, we found that the incorporation of PDA on CNTs can also effectively avoid the interference of the reaction between -NCO and -OH by pristine CNTs. It is believed that the combination of these factors is responsible for the significant improvement of mechanical properties. The PDA-CNTs are promising candidates for use as fillers to prepare PU nanocomposites with high mechanical properties at low CNTs loadings.

References

[1] Ruoff RS, Lorents DC. Carbon 1995;33:925-30.

[2] Ajayan PM, Stephan O, Colliex C, Trauth D. Science 1994;265:1212-4.

[3] Calvert P. Nature 1999;399:210-1.

[4] Spitalsky Z, Tasis D, Papagelis K, Galiotis C. Prog. Polym. Sci. 2010;35:357-401.

[5] Han Z, Fina A. Prog. Polym. Sci. 2011;36:914-44.

[6] Ma P-C, Siddiqui NA, Marom G, Kim J-K. Composites Part A 2010;41:1345-67.

[7] Bokobza L. Polymer 2007;48:4907-20.

[8] Kim B-S, Kim D, Kim K-W, Lee T, Kim S, Shin K, Chun S, Han JH, Lee YS, Paik H-j.
Carbon 2014;72:57-65.

[9] Yu J, Grossiord N, Koning CE, Loos J. Carbon 2007;45:618-23.

[10] Waite JH, Tanzer ML. Science 1981;212:1038-40.

[11] Lee H, Dellatore SM, Miller WM, Messersmith PB. Science 2007;318:426-30.

[12] Zhang R, Su Y, Zhao X, Li Y, Zhao J, Jiang Z. J. Membr. Sci. 2014;470:9-17.

[13] Gu R, Xu WZ, Charpentier PA. Polymer 2014;55:5322-31.

[14] Ye W, Chen Y, Zhou Y, Fu J, Wu W, Gao D, Zhou F, Wang C, Xue D. Electrochim. Acta
2014;142:18-24.

[15] Zhu B, Edmondson S. Polymer 2011;52:2141-49.

[16] Dalsin JL, Hu B-H, Lee BP, Messersmith PB. J. Am. Chem. Soc. 2003;125:4253-58.

[17] Cheng XQ, Zhang C, Wang ZX, Shao L. J. Membr. Sci. 2016;499:326-34.

[18] Quan S, Li S, Wang Z, Yan X, Guo Z, Shao L. J. Mater. Chem. A 2015;3:13758-66.

[19] Wang Z, Xu Y, Liu Y, Shao L. J. Mater. Chem. A 2015;3:12171-8.

[20] Fei B, Qian B, Yang Z, Wang R, Liu WC, Mak CL, Xin JH. Carbon 2008;46:1795-97.

[21] Jiang Y, Lu Y, Zhang L, Liu L, Dai Y, Wang W. J. Nanopart.Res. 2012;14:1-10.

[22] Yoon TH, Park YJ. J. Power Sources 2013;244:344-53.

[23] Shi C, Deng C, Zhang X, Yang P. ACS Appl. Mater. Interfaces 2013;5:7770-76.

[24] Subramanian AS, Tey JN, Zhang L, Ng BH, Roy S, Wei J, Hu X. Polymer 2016;82:285-94.

[25] Chattopadhyay DK, Raju KVSN. Prog. Polym. Sci. 2007;32:352-418.

[26] Hu H, Yu B, Ye Q, Gu Y, Zhou F. Carbon 2010;48:2347-53.

20

[27] Zhang L, Roy S, Chen Y, Chua EK, See KY, Hu X, Liu M. ACS Appl. Mater. Interfaces 2014;6:18644-52.

[28] Hood MA, Gold CS, Beyer FL, Sands JM, Li CY. Polymer 2013;54:6510-15.

[29] Chen S, Wu G, Liu Y, Long D. Macromolecules 2005;39:330-4.

[30] Roy S, Das T, Yue CY, Hu X. ACS Appl. Mater. Interfaces 2013;6:664-70.

[31] Zangmeister RA, Morris TA, Tarlov MJ. Langmuir 2013;29:8619-28.

[32] Ma J, Zhang S, Qi Z. J. Appl. Polym. Sci. 2001;82:1444-8.

[33] Kim JA, Seong DG, Kang TJ, Youn JR. Carbon 2006;44:1898-905.

[34] Woods LM, Bădescu ŞC, Reinecke TL. Phys. Rev. B 2007;75:155415.

[35] Goclon J, Kozlowska M, Rodziewicz P. Chem. Phys. Lett. 2014;598:10-6.

[36] Xu M, Zhang T, Gu B, Wu J, Chen Q. Macromolecules 2006;39:3540-45.

[37] Kwon J, Kim H. Journal of Polymer Science Part A: Polym. Chem. 2005;43:3973-85.

[38] Kuan H-C, Ma C-CM, Chang W-P, Yuen S-M, Wu H-H, Lee T-M. Compos. Sci. Technol. 2005;65:1703-10.

[39] Hu X, Stanford JL, Day RJ, Young RJ. Macromolecules 1992;25:672-83.

[40] Wang G, Fang B, Zhang Z. Polymer 1994;35:3178-83.

[41] Zhang C, Ren Z, Yin Z, Qian H, Ma D. Polym. Bull. 2008;60:97-101.

[42] Lee HS, Wang YK, MacKnight WJ, Hsu SL. Macromolecules 1988;21:270-73.

[43] Pavličević J, Špírková M, Bera O, Jovičić M, Pilić B, Baloš S, Budinski-Simendić J. Composites Part B 2014;60:673-9.

[44] Affdl JCH, Kardos JL. Polym. Eng. Sci.1976;16:344-52.

[45] Schaefer DW, Justice RS. Macromolecules 2007;40:8501-17.

[46] Kim M, Park Y-B, Okoli OI, Zhang C. Compos. Sci. Technol. 2009;69:335-42.

[47] Yu M-F, Lourie O, Dyer MJ, Moloni K, Kelly TF, Ruoff RS. Science 2000;287:637-40.

[48] Morimune S, Nishino T, Goto T. Polym. J 2012;44:1056-63.

[49] Liang J, Huang Y, Zhang L, Wang Y, Ma Y, Guo T, Chen Y. Adv. Funct. Mater. 2009;19:2297-302.

- Pristine CNTs was successfully modified by PDA through self-oxidative polymerization

- The presence of PDA coating facilitated uniformly CNTs dispersion in PU matrix and created strong interfacial interaction between CNTs and PU matrix

- PDA-CNTs increased the phase separation and induced a structural change of PU.

- 40% increase in tensile modulus and 100% increase in tensile strength were achieved with a loading of only 0.3 wt% PDA-CNTs.

- The reinforcement by PDA-CNTs exceeded the predicted modulus by Halpin-Tsai model by ~29% at 0.3 wt% of PDA-CNTs loading.